

**EFFECTS OF CURRENT DENSITY, ETCHING TIME AND
HYDROFLUORIC ACID CONCENTRATION ON THE FORMATION AND
MORPHOLOGY OF HIGHLY DOPED N-TYPE POROUS SILICON**

by

SURIANI BINTI HAJI YAAKOB

Thesis submitted in fulfilment of the requirements

for the degree of Master of Science

July 2011

**EFFECTS OF CURRENT DENSITY, ETCHING TIME AND
HYDROFLUORIC ACID CONCENTRATION ON
THE FORMATION AND MORPHOLOGY OF HIGHLY DOPED
N-TYPE POROUS SILICON**

SURIANI BINTI HAJI YAAKOB

UNIVERSITI SAINS MALAYSIA

2011

ACKNOWLEDGEMENT

I would like to take this opportunity to thank many people who have made it possible for me to complete this thesis. Firstly, my appreciation goes to my main supervisors, Prof Dr. Mohamad Abu Bakar for his support, guidance and advice throughout of the completion of this work. His patience and generosity have always been admired. Also, thank you to my co-supervisor, Prof Kamarul Azizi Ibrahim who gave me permission to use the facilities in NanoOptoelectronic Research and Technology (NOR) Lab. In addition, a special thanks to Prof. Dr. Jamil Ismail for his encouragement, motivation and guidance all these years.

My gratitude also goes to Mr. Mohtar Sabdin, Mr. Abdul Jamil, Mr. Hazhar and Mss. Bee Choo (School of Physics), Miss Jamilah, Mr. Johari (School of Biological Sciences), Mr. Abdul Rashid, Mr. Mohd. Azam (School of Materials and Mineral Resources Engineering), Mr. Ali and other member of the staff of School of Chemical Sciences for their assistance and co-operation.

Last but not least, I would like to thank my family for their encouragement and support that they have given to me all along the long journey. I am also truly deeply blessed to have my good friend Nor Hashila Mohd Hirmizi, Yeo Siew Yean, Noorul Ain Mohd Akib, Hanani Yazid, Dr. Noor Hana Hanif Abu Bakar, Tan Wei Leng, Rosniza Hamzah and Atoosa Haghighizadeh for helping me a lot throughout my research. Thank you to all of you.

Suriani Binti Haji Yaakob

July 2011

CONTENTS

ACKNOWLEDGEMENTS	ii
CONTENTS	iii
LIST OF TABLES	viii
LIST OF FIGURES	ix
ABBREVIATIONS	xiii
LIST OF SYMBOL	xv
ABSTRAK	xvi
ABSTRACT	xvii

CHAPTER 1 - INTRODUCTION

1.1	A Brief Overview	1
1.2	Problem Statements	2
1.3	Aims	3
1.4	Objectives	3
1.5	Scope of Study	3
1.6	Thesis Layout	4

CHAPTER 2 - LITERATURE REVIEWS

2.1	Introduction	5
2.2	Silicon Substrates for PS	5
2.2.1	n-type Si	6
2.2.2	p-type Si	7
2.3	Porous Silicon (PS)	7
2.4	Morphological Characteristics of PS	10
2.5	Methods of PS Fabrications	13

2.6	PS Formations via Electrochemical Etching	14
2.6.1	Principles PS Formations	15
2.6.1.1	Etching Reactions	15
2.6.1.2	Direct Dissolution	16
2.6.1.3	Indirect Dissolution	17
2.6.1.4	Critical Current Density (J_{PS})	18
2.6.1.5	Electro-polishing	19
2.6.2	Si-electrolyte Interface	19
2.6.3	Parameters Controlling the PS Formations	22
2.6.3.1	Current Density	22
2.6.3.2	Etching Time and HF Concentration	22
2.6.3.3	Temperature and pH of Electrolyte	24
2.6.3.4	Types of Dopant, Dopant Loading and Illumination	25
2.6.3.5	Si Orientation	25
2.6.4	Properties of PS Formed by Electrochemical Etching	25
2.6.4.1	Crystal Structure	25
2.6.4.2	Chemical Properties	26
2.6.4.3	Electrical Properties	27
2.6.4.4	Thermal Conductivity	28
2.6.4.5	Optical Properties	28
2.6.4.6	Mechanical Properties	29
2.7	Applications of PS	30
2.7.1	Opto-electronic Device	30
2.7.2	Biomedical Device	31
2.7.3	Sensor	31
2.7.4	Host for Metal Deposition	32
2.8	Metal Deposition onto PS	32
2.8.1	Deposition via Immersion Plating	33
2.8.2	The Parameters of the Deposition Process	34

2.8.3	The Current Issues of Metal Deposition by Immersion Plating	37
-------	---	----

CHAPTER 3 - MATERIALS AND EXPERIMENTAL METHODS

3.1	Materials	38
3.2	Method	38
3.2.1	PS formations	38
3.2.1.1	Pre-treatments of Si Wafers	39
3.2.1.2	Electrochemical Etching	40
3.2.2	Copper Deposition onto PS via Immersion Plating	41
3.3	Characterizations	41
3.3.1	Scanning Electron Microscopy (SEM) and Energy Dispersive X-ray Analysis (EDX)	41
3.3.2	Gravimetric Method	42
3.3.3	Atomic Force Microscopy (AFM)	43
3.3.4	Current-voltage (I-V) Characteristics	43
3.3.5	Optical microscopy	44
3.3.6	X-ray Diffraction (XRD)	44

CHAPTER 4 - EFFECT OF CURRENT DENSITY ON THE FORMATION OF POROUS SILICON

4.1	Introduction	45
4.2	Cross-sectional Morphology of PS Layer	45
4.3	Thickness of PS Layer	53
4.4	Surface Morphology of PS Layer	54
4.5	Porosity of PS Layer	56
4.6	Surface Roughness of PS Layer	57
4.7	Electrical Properties of PS Layer	59
4.8	Summary	60

CHAPTER 5 - EFFECT OF ETCHING TIME ON THE FORMATION

OF POROUS SILICON

5.1	Introduction	62
5.2	Cross-sectional Morphology of PS Layer	62
5.3	Thickness of PS Layer	65
5.4	Surface Morphology of PS Layer	66
5.5	Porosity of PS Layer	69
5.6	Surface Roughness of PS Layer	70
5.7	Electrical Properties of PS Layer	72
5.8	Summary	73

CHAPTER 6 - EFFECT OF HF CONCENTRATION ON THE FORMATION OF POROUS SILICON

6.1	Introduction	75
6.2	Cross-sectional Morphology of PS Layer	75
6.3	Thickness of PS Layer	81
6.4	Surface Morphology of PS Layer	83
6.5	Porosity of PS Layer	87
6.6	Surface Roughness of PS Layer	88
6.7	Electrical Properties of PS Layer	91
6.8	Summary	93

CHAPTER 7 - DEPOSITION OF COPPER ONTO POROUS SILICON

7.1	Introduction	94
7.2	Formation of Cu onto the PS	94
7.3	XRD Analysis of Cu-PS	95
7.4	Effect of Immersion Time	95
7.4.1	Morphology and the Average Particle Size of Cu-PS	95
7.4.2	EDX Analysis of Cu-PS	99
7.4.3	Cross-sectional Morphology and Thickness of Cu Layer	100

7.4.4	Topography and Surface Roughness of Cu-PS	103
7.5	The Effect of MEK on Metal Deposition on PS surface	105
7.5.1	Morphology and the Average Particle Size of Cu-PS	105
7.5.2	EDX Analysis of Cu-PS	107
7.5.3	Cross-sectional Morphology and Thickness of Cu layer	109
7.5.4	Topography and Surface Roughness of Cu-PS	112
7.6	Summary	112
 CHAPTER 8 - CONCLUSION		
8.1	Conclusion	115
8.2	Recommendations for Future Work	117
 REFERENCE		119
LIST OF PUBLICATIONS AND PRESENTATIONS AT CONFERENCES		140

LIST OF TABLES

Table 2.1	Morphological characteristics of PS	12
Table 3.1	Basic parameters used for PS formation.	40

LIST OF FIGURES

Figure 2.1	Simplified energy band in pure Si crystal	6
Figure 2.2	Energy band in n-type Si	8
Figure 2.3	Energy band in p-type Si	8
Figure 2.4	Morphological characteristic of PS	11
Figure 2.5	Reaction scheme of PS formation via direct dissolution	17
Figure 2.6	Reaction scheme of PS formation via indirect dissolution	18
Figure 2.7	Schematic illustration of the double layers in the semiconductor-electrolyte interface at an equilibrium condition.	20
Figure 2.8	Types of space charge layers on n-type Si surface; (a) depletion, (b) inversion and (c) accumulation layer	21
Figure 3.1	Procedures of PS formations	39
Figure 3.2	Experimental set-up of PS formations	41
Figure 3.3	Top view of PS sample for I-V characteristics measurements	44
Figure 3.4	Experimental set-up for I-V characteristics measurements	44
Figure 4.1	SEM image of a typical cross-section PS layer on bulk Si	46
Figure 4.2	SEM images of cross-sections at various locations in the PS layers, i.e. entry, middle and bottom regions prepared at current densities of (a) 50, (b) 100, (c) 200 and (d) 300 mA cm ⁻²	47
Figure 4.3	The formation of interconnected network morphology in PS.	49
Figure 4.4	The formation of (a-c) columnar in <100> plane, branching in <111> plane and (d) wider and unbranched pore channel with increasing depth	51
Figure 4.5	SEM images of cross-section of an electro-polished PS layer prepared at a current density of 305 mA cm ² and	52

	the inset represents the enlargement of area 1	
Figure 4.6	Plots of lateral thickness (◆) and etch rate (▲) as a function of current density	53
Figure 4.7	SEM surface images of PS prepared at current densities of (a) 50, (b) 100, (c) 200 and (d) 300 mA cm ⁻²	54
Figure 4.8	Plots of the average pore diameter (●) and pore density (■) as a function of current density	55
Figure 4.9	The scheme for holes accumulation and distribution on Si surface during PS formation; (a) random distribution of collective holes at low current density, (b) holes accumulate as the current density increases, (c) merging of the neighbouring pores resulting in the large pore at high current density	56
Figure 4.10	Plot of porosity as a function of current density	57
Figure 4.11	AFM topographs of (a) bulk Si and PS formed at current density of (b) 50, (c) 150 and (d) 300 mA cm ⁻²	58
Figure 4.12	Plot of surface roughness as a function of current density	59
Figure 4.13	I-V characteristics of the Al/Si/Al and Al/PS/Si/Al as a function of current density	60
Figure 5.1	SEM images of cross-sections of PS prepared at different etching time of (a) 30 s, (b) 90 s, (d) 180 s and (e) 300 s	63
Figure 5.2	Plots of lateral thickness (◆) and etch rate (○) as a function of etching time	66
Figure 5.3	SEM surface images of PS prepared at etching time of (a) 30 s, (b) 90 s, (c) 180 s and (d) 300 s	67
Figure 5.4	Plots of the average pore diameter (◆) and pore density (△) as a function of etching time	68
Figure 5.5	Plot of inter-pore distance as a function of etching time	69
Figure 5.6	Plot of porosity as a function of etching time	70
Figure 5.7	AFM topographs of (a) bulk Si and PS surface formed using different etching time of (b) 30 s, (c) 60 s, (d) 90 s, (e) 180 s and (f) 300 s	71
Figure 5.8	Plot of surface roughness as a function of etching time	72
Figure 5.9	I-V characteristics of the Al/Si/Al and Al/PS/Si/Al as a function of etching time	73
Figure 6.1	Optical microscope images of the surface of bulk Si and PS formed at 300 mA cm ⁻² using various (v/v) HF	76

	concentrations. (Mag = 5k)	
Figure 6.2	Optical microscope images of the surface of bulk Si and PS formed at 150 mA cm ⁻² using various (v/v) HF concentrations. (Mag = 5k)	77
Figure 6.3	SEM images of cross-sections of PS layer formed using various (v/v) HF concentrations at current density of 300 mA cm ⁻² ; (a) 24.5% (b) 29.4% (c) 34.3% and (d) 39.2%	79
Figure 6.4	SEM images of cross-sections of PS layer formed using various (v/v) HF concentrations at current density of 150 mA cm ⁻² ; (a) 19.6%, (b) 29.4%, (c) 39.2% and (c) 49.0%	80
Figure 6.5	Plots of lateral thickness (◆) and etch rate (▲) as a function of HF concentration at constant current density of 300 mA cm ⁻²	82
Figure 6.6	Plots of lateral thickness (○) and etch rate (●) as a function of HF concentration at constant current density of 150 mA cm ⁻²	82
Figure 6.7	SEM surface images of PS prepared at (a) 24.5% (b) 29.4% (c) 34.3% and (d) 39.2% HF concentration at current density of 300 mA cm ⁻²	84
Figure 6.8	SEM surface images of PS prepared at (a) 19.6%, (b) 29.4%, (c) 39.2% and (c) 49.0% (v/v) HF concentration at current density of 150 mA cm ⁻²	84
Figure 6.9	Plots of the average pore diameter (◆) and pore density (▲) as a function of HF concentration at current density of 300 mA cm ⁻² current density	86
Figure 6.10	Plots of the average pore diameter (◆) and pore density (●) as a function of HF concentration at current density of 150 mA cm ⁻² current density	86
Figure 6.11	Plots of porosity against HF concentration at 300 mA cm ⁻² (◆) and 150 mA cm ⁻² (▲)	87
Figure 6.12	AFM topographs of PS surface prepared using various (v/v) HF concentrations; (a) 24.5%, (b) 29.4, (c) 34.3% and (d) 39.2% at current density of 300 mA cm ⁻²	89
Figure 6.13	AFM topographs of PS surface prepared using various (v/v) HF concentrations; (a) 19.6, (b) 29.4, (c) 39.2 and	90

(d) 49.0% at current density of 150 mA cm^{-2}

Figure 6.14	Plots of surface roughness as a function of HF concentration at current density 300 mA cm^{-2} (▲) and 150 mA cm^{-2} (□)	91
Figure 6.15	I-V characteristics of the Al/Si/Al and Al/PS/Si/Al as a function of HF concentration at 300 mA cm^{-2} current density	92
Figure 6.16	I-V characteristic of Al/Si and Al/PS/Si/Al as a function of HF concentration at 150 mA cm^{-2} current density	92
Figure 7.1	Typical XRD patterns of (a) PS, (b) Cu-PS prepared using CuSO_4 solution and (c) Cu-PS prepared using a mixture of CuSO_4 and MEK with a ratio of 1:1.	96
Figure 7.2	SEM surface images and size distribution histograms of Cu-PS prepared using 0.001 M CuSO_4 solution for (a) 30, (b) 120 and (c) 420 min	97
Figure 7.3	The weight (%) of copper (Cu) and oxygen (O) elements obtained from EDX analysis of Cu-PS prepared using 0.001 M CuSO_4 solution at (a) 30, (b) 120 and (c) 420 min of immersion time	100
Figure 7.4	(a) SEM image of cross-section and (b) EDX spectrum of area 1 of Cu-PS prepared at 30 min of immersion time	101
Figure 7.5	Plots of thickness of Cu layer on PS surface (◆) and thickness of Cu layer in pore entry (●) as a function of immersion time	102
Figure 7.6	AFM topographs of (a) PS and Cu-PS surface formed at (b) 30 min, (c) 120 min and (d) 420 min of immersion time	104
Figure 7.7	SEM surface images and size distribution histograms of Cu-PS prepared using a mixture of MEK and CuSO_4 with ratio 1:1 (v/v) for (a) 30, (b) 120 and (c) 420 min of immersion time	106
Figure 7.8	The weight (%) of Cu and O elements obtained from EDX analysis of Cu-PS prepared using a mixture of MEK and CuSO_4 with ratio 1:1 (v/v) for the immersion time of (a) 30, (b) 120 and (c) 420 min	108
Figure 7.9	(a) SEM image of cross-sectional and (b) EDX spectrum of area 2 of Cu-PS prepared using a mixture of MEK and CuSO_4 with ratio 1:1 (v/v) for 30 min immersion time	110
Figure 7.10	Plots of thickness of Cu layer on PS surface (◆) and	111

thickness of Cu layer in pore entry (●) as a function of immersion time

Figure 7.11 AFM topographs of Cu-PS surface formed at (a) 30 min, 113
(b) 120 min and (c) 420 min of immersion time

ABBREVIATIONS

AFM	Atomic Force Microscopy
CCP	Capacitive Coupled Plasma
Cu-PS	Copper-deposited Porous Silicon
DC	Direct current
DRIE	Deep Reactive Ion Etching
E_g	Energy Gap
ERDA	Elastic Recoil Detection Analysis
Fcc	Face-centered cubic
ICDD	International Centre Diffraction Data
ICP	Inductive Coupled Plasma
IHP	Inner Helmholtz Plane
IR	Infra-red
I-V	Current-Voltage
J_{PS}	Critical Current Density
MEK	Methyl Ethyl Ketone
OHP	Outer Helmholtz Plane
PL	Photoluminescence
PS	Porous Silicon
r.m.s	Root Mean Square
RCA	Radio Corporation of America
SCR	Space Charge Region
SD	Standard Deviation
SEM	Scanning Electron Microscopy
SIMS	Secondary Ion Mass Spectrometry
XRD	X-ray Diffraction

LIST OF SYMBOLS

A	Ampere
eV	electron Volt
kV	kilo Volt
M	Molar
mA	mili Ampere
min	Minute
s	second
v/v	volume to volume ratio
Ω	Ohm

**KESAN KETUMPATAN ARUS, MASA PUNARAN DAN KEPEKATAN ASID
HIDROFLUORIK TERHADAP PEMBENTUKAN DAN MORFOLOGI
SILIKON BERLIANG PENDOPAN JENIS-N YANG TINGGI**

ABSTRAK

Silikon berliang (PS) pendopan jenis-n yang tinggi telah disediakan melalui punaran elektrokimia. Kesan ketumpatan arus ($50 - 300 \text{ mA cm}^{-2}$), masa punaran ($30 - 300 \text{ s}$) dan kepekatan asid hidrofluorik (HF) ($9.2 - 49.0 \% \text{ (v/v)}$) terhadap morfologi, diameter liang, keliangan, kekasaran permukaan dan sifat elektrik PS telah dikaji. Sifat-sifat ini dicirikan melalui Mikroskop Pengimbasan Elektron (SEM), kaedah gravimetri, Mikroskop Daya Atom (AFM), dan pencirian Arus-Voltan (I-V). Peningkatan ketumpatan arus telah mengubah morfologi PS dari jaringan saling tersambung kepada turus bercabang tepi. Manakala, dengan peningkatan masa punaran dan kepekatan HF, liang dinding bertepi licin terhasil. Diameter liang bertambah dengan pertambahan ketumpatan arus, tetapi berkurang dengan kepekatan HF dan kekal konsisten pada $19.0 \pm 2.8 \text{ nm}$ dengan masa punaran. Keliangan PS bertambah dengan peningkatan ketumpatan arus dan masa punaran, tetapi berkurang dengan kepekatan HF. Suatu nilai optimum kekasaran permukaan, pada ketumpatan arus 150 mA cm^{-2} dan masa punaran 180 s diperoleh dalam semua julat parameter yang dikaji. Manakala, kecenderungan penurunan diperhatikan dengan peningkatan kepekatan HF. Sifat elektrik PS juga berkurang dengan peningkatan keliangan dalam semua keadaan yang dikaji. Pengelektro-gilapan berlaku pada ketumpatan arus $> 300 \text{ mA cm}^{-2}$ dan masa punaran $> 300 \text{ s}$. Pemerhatian yang sama berlaku pada kepekatan HF yang rendah iaitu $9.2\% \text{ (v/v)}$ dengan ketumpatan arus 150 mA cm^{-2} dan kepekatan HF pada $19.6\% \text{ (v/v)}$ dengan ketumpatan arus 300 mA cm^{-2} . PS yang diperoleh juga digunakan sebagai perumah pengendapan logam kuprum (Cu) melalui penyadur rendaman. Keputusan SEM menunjukkan morfologi zarah-zarah Cu berubah dari bentuk kiub kepada sfera padat-rapat dengan penambahan $1:1 \text{ (v/v)}$ metil etil keton (MEK) ke dalam larutan garam Cu (0.001 M) sebelum proses rendaman. Proses ini meningkatkan litupan zarah-zarah Cu ke atas permukaan PS dibandingkan proses rendaman menggunakan

garam Cu sahaja. Saiz zarah-zarah Cu juga dikawal dengan mempelbagaikan masa punaran.

EFFECTS OF CURRENT DENSITY, ETCHING TIME AND HYDROFLUORIC ACID CONCENTRATION ON THE FORMATION AND MORPHOLOGY OF HIGHLY DOPED N-TYPE POROUS SILICON

ABSTRACT

Highly doped n-type porous silicons (PS) were prepared via electrochemical etching. The effect of current density ($50 - 300 \text{ mA cm}^{-2}$), etching time ($30 - 300 \text{ s}$) and HF concentration ($9.2 - 49.0\% \text{ (v/v)}$) on the morphology, pore diameter, porosity, surface roughness and electrical properties of the PS were studied. These properties were characterized by Scanning Electron Microscopy (SEM), gravimetric method, Atomic Force Microscopy (AFM) and Current-Voltage (I-V) characteristics. The increment in current density has changed the morphology of the PS from interconnected network to columnar with side branching. However, with the increase in the etching time and HF concentration, this disappeared to give smooth side wall pores. The pore diameter increased with increase in current density, but decreased with HF concentration and remained consistent at $19.0 \pm 2.8 \text{ nm}$ with the etching time. The porosity of PS was increased with increase in current density and etching time, but decreased with the HF concentration. An optimum value of the surface roughness at 150 mA cm^{-2} of current density and 180 s of etching time was obtained in all ranges of parameters studied. However, a decreasing trend was observed with the increase in HF concentration. The electrical properties of PS also decreased with the increase in porosity in all studied conditions. The electro-polishing was found to occur at current density $> 300 \text{ mA cm}^{-2}$ and etching time $> 300 \text{ s}$. Similar observations on the PS formed at low HF concentration of $9.2\% \text{ (v/v)}$ and current density of 150 mA cm^{-2} as well as that formed in $19.6\% \text{ (v/v)}$ HF at 300 mA cm^{-2} were obtained. The obtained PS was also employed as a host for metallic copper (Cu) deposition by immersion plating. The SEM results showed that the morphology of Cu particles changed from cubes to close-pack spheres upon addition of $1:1 \text{ (v/v)}$ methyl ethyl ketone (MEK) into the Cu salt (0.001 M) solution prior to immersion

process. This improved the Cu particles coverage onto the PS surface compared to immersion process using Cu salt solely. The size of Cu particles was controllable by varying the immersion time.

CHAPTER 1

INTRODUCTION

1.1 A Brief Overview

Porous silicon (PS) has become one of the highly attractive materials upon the demonstration of its photoluminescence and electroluminescence properties in the 1990s [1, 2]. Since then, it has received increasing attention and has been widely investigated due to its potential in various fields including catalysis, optoelectronics, biotechnology, and sensor devices. The above range of properties is attributed to different morphologies exhibited by the PS. A wide range of morphologies have been reported ranging from array of columnar to high porosity interconnected networks with pore sizes ranging from macro to nano scale. Combination of nano-size pores and high porosity of the interconnected networks delivers photoluminescence and electroluminescence properties associated with quantum size effect. Electrochemical etching is the most widely used technique in producing PS and the morphology of PS is controlled by the various parameters involved. In order to realize applications potentials, good understanding of mechanism and principles are crucial to the control of the formation and reproduction of PS. The fabrication of PS is converging on the nanometer scale that will open the door to nanotechnology and motivates research on PS as an advanced material to meet the energy, environmental and health challenges.

Both p- and n-types silicon (Si) are interesting to study as they give a wide range of morphologies. Typically, p-type PS gives macro-size to nano-size interconnected networks with high porosity. This morphology demonstrates good photoluminescence (PL) properties and therefore has inspired many researchers to carry out studies using this type of Si [3-10]. On the other hand, detailed study of n-

type Si is limited. However, this type of Si has been shown to form columnar structures with low porosity although revealing less of the PL properties. Nonetheless, there is a possibility of modifying and controlling the PS morphology as well as the pore size by adjusting the parameters involved. Therefore, one must understand clearly the basic mechanisms and principles of PS formations.

1.2 Problem Statements

- Morphology and size control of PS has gained enormous attention due to its unique properties that are often associated with its varied morphologies. One of the main challenges is to control its pore structures and size for specific properties and applications. PS formations via electrochemical method involve many parameters thus understanding the physical and chemical aspects of the process are vital.
- To date, the principles and mechanisms of PS formations available cannot provide a complete description of the reactions occurring at the Si electrode leading to varieties of morphology. The details of anodic electrochemical reactions and dissolution processes at the Si-electrolyte interface are still not fully understood.
- It is well known that one of the interesting properties exhibited by the PS is its ability to reduce metal ions to metal. Due to this, PS has potential to be employed as a host for metal deposition. The simplest deposition technique is via immersion plating. However, the nature of the reduction process and the control of deposited metal morphology need further understanding.

1.3 Aims

The aims of the study is to optimize the formations of PS using electrochemical technique, focusing on the effects of current density, etching time and HF concentration using highly doped n-type Si and utilizing the reducing property of the prepared PS to coat metallic layer on the PS using the simplest technique i.e. immersion plating.

1.4 Objectives

The objectives of this study are as follows:

- To prepare the PS by electrochemical method.
- To vary the current density, etching time and HF concentration to control the morphology of PS obtained.
- To characterize the obtained PS using SEM, AFM, Gravimetric and Current-Voltage (I-V) characteristics measurements system.
- To apply the pre-formed PS as a host for metal deposition using immersion plating technique.

1.5 Scope of Study

This study is limited to the fabrication of PS from n-type Si using an electrochemical technique and looking into the effect of current density, etching time and HF concentration. Upon characterization of the physical properties of PS, investigations into electrical properties are conducted. Besides, the optimum parameters are sought in preparing PS which meets the desired structure. Furthermore, the obtained PS was applied as a host for copper deposition. The deposition process is via the immersion plating technique.

1.6 Thesis Layout

This thesis comprises of 8 chapters. The first chapter is an introduction to this thesis. It gives an overview of PS, problem statements and justification, the aims and objectives as well as the scope of this study. Chapter 2 presents a literature review, which covers the basic mechanisms and principles of PS formations, morphologies, properties, fabrication techniques and its various applications. Meanwhile, Chapter 3 provides detailed experimental procedures and techniques. The effect of different current densities on the formation of PS is discussed comprehensively in Chapter 4. Chapter 5 and 6 report about the effect of etching times and HF concentrations, respectively. For application purpose, the obtained PS has been used as a host for deposition of metallic copper. This is discussed in Chapter 7. Finally, Chapter 8 will conclude this investigation and provide some recommendations for future works.

CHAPTER 2

LITERATURE REVIEW

2.1 Introduction

In general, this chapter concerns on literature review of PS, its formation and applications. The obtained morphology of the n- or p-type PS may differ with the methods of fabrication. One of the methods that have been widely used in producing PS is the electrochemical etching. Via this method, the related principles of PS formation, the processes that occur at the Si-electrolyte interface, the parameters that control the formation of PS and the properties of the formed PS are discussed comprehensively. In addition, the applications of PS also are reviewed in this chapter.

2.2 Silicon Substrates for PS

Silicon is a chemical element, which has the symbol Si and atomic number 14. It is a semiconductor material with conductivity between the conductor and insulator [11]. The simplified energy band of pure Si crystal is depicted in Figure 2.1. As the energy gap (E_g) between conduction band and valence band is comparable to thermal energy (ambient), some electrons will be excited from valence band to the conduction band. The excitation of electrons leaves behind vacant places known as holes in the valence band. The number of holes in the valence band is equal to the number of excited electrons in the conduction band. Moreover, both the conduction band electrons and the valence band holes contribute to electrical conductivity. In fact, the holes themselves do not move, but a neighbouring electron can move to fill in the hole. As a result, it leaves a hole at the place it has just come from. In this way,

the holes appear to move. The conductivity of Si increases with impurities in the crystal lattice. A semiconductor whose conductivity is significantly affected by impurities is called extrinsic semiconductor. Extrinsic semiconductors are made up of different dopant types leading to two general types namely n- and p-type Si.

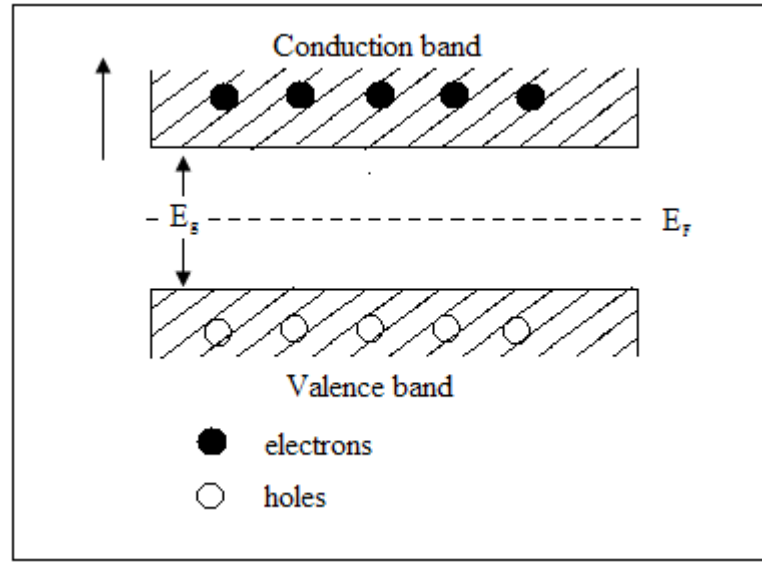


Figure 2.1: Simplified energy band in pure Si crystal [11].

2.2.1 n-type Si

This material comprises donor impurities atoms in the Si crystal lattice. These donor atoms are from group 15 of the Periodic Table such as either phosphorus (P), germanium (Ge) or arsenic (As). The diagram of n-type energy band is given in Figure 2.2. The presence of donor atoms in crystal lattice of Si provides more valence electrons than required to complete the bond between neighbouring Si atoms. Therefore, it affects the distribution of energy and forms an extra level close to the conduction band. Donor atom gives up their electrons to the conduction band easily and therefore it is ionized. In this type of Si, the number of conduction electron is greater than the mobile holes.

2.2.2 p-type Si

Figure 2.3 shows the energy band in p-type Si. In this type of Si, typical acceptor impurity atoms are boron (B), Aluminium (Al), or Gallium (Ga). Elements from group 13 of the Periodic Table having fewer valence electrons than required to form bonds with neighbouring Si atoms. They accept electrons from any source to complete the bonds. Thus, an energy level just above valence band is created. Therefore, electron in the valence band just needs smaller increment of energy to occupy the acceptor level and leaving behind holes. The excited electrons are bound to the acceptor atom resulting in ionized dopant. In this type of Si, the number of holes becomes dominant.

2.3 Porous Silicon (PS)

PS was first discovered by Uhler in 1956 [12] while performing an electrochemical etching of Si electrode in HF electrolyte. Details of PS formation were further investigated by Turner in 1958 [13]. In their works, they have found that the Si surface was covered with a brown film after the etching process. They suggested that the film was a subfluoride $(\text{SiF}_2)_x$ grown on the substrate. On the other hand, in 1966, Memming and Schawndt [14] proposed that the brown film was a precipitation product (Si^0 amorphous) resulting from the etching process. In the early 1970s, there were a few reports on the formation of etch pits and tunnels on n-type Si [15, 16]. It was also established that the solid surface layer is the remaining Si substrate left after anodic dissolution.

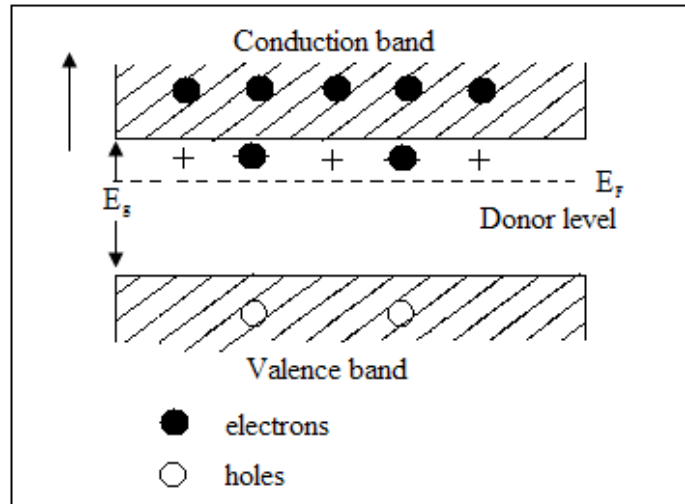


Figure 2.2: Energy band in n-type Si [11].

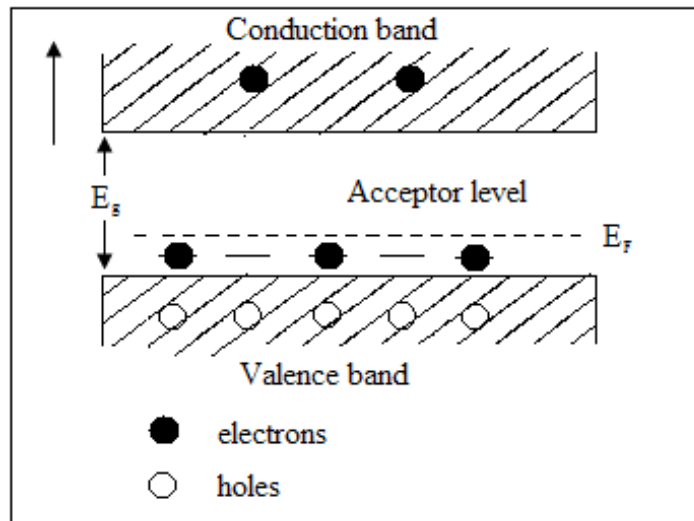


Figure 2.3: Energy band in p-type Si [11].

Later, a crystallinity study of the PS material was discussed by Arita et al. [17] and Watanabe et al. [18]. It was established that the brown film formed by anodization on Si substrate of all types of Si is a porous with the same single crystalline structure as a substrate. Afterwards, Lehmann et al. [2] have reported the formation of straight, smooth and well spaced macro pore arrays on n-type Si using surface patterning and backside illumination [19, 20]. Accordingly, for these large

straight pores, the dissolution rate at the pore tips is limited by mass transfer in the electrolyte. Moreover, the PS morphology is determined by the relative rates of carrier transport in the Si and mass transport in the electrolyte. Meanwhile, Canham [1] has reported the visible PL effect shown by high porosity of PS at room temperature. This result has stimulated great interest because of the potential of a Si-based optoelectronics. Since then, many attempts were made to modify the morphology of PS that leads to new properties of PS. In 1992, PS with pore directed along $\langle 100 \rangle$ on different types of Si has been identified by Smith et al. [21]. Two years after, the formation of branching at the main pores of n-type Si was reported by Takemoto et al. [22]. In addition, Propst and Kohl [23] have reported the formation of macro-PS on low doped p-type Si. A study of the condition for the formation of macropores on p-type Si in different mixture of aqueous HF and organic solvents was also reported by Lust and Clement [24]. In 2003, Zvalioniene et al. [25] have reported the formation of porous structure comprising dense branched network at low current density. However, the pore morphology tends to be anisotropy with increasing current density. Matthias et al. [26] in 2005 tried to control the non-uniformity in macro PS growth of n-type Si. The macro PS etching was initiated by a non-uniform predefined lattice. In their work, they have observed the stable growth of pores whose geometrical appearance depends strongly on the spatially different nucleation conditions. In the same year, the enhanced control of PS morphology from macro to meso-pores formation of n-type Si was reported by Ouyang et al. [27]. Meanwhile, Bao et al. [28] in 2007 improved the speed of pore formation by introducing strong oxidizers in the electrolyte solution. Recently, in 2009, an experimental study of macro pore formation on p-type Si has been conducted to

study the transition between macro pore formation and electro-polishing [29]. It should be noted that the report concerning the same issue for n-type Si is scarce.

Based on this review, it is noted that issues on controlling PS's morphology are still challenging. Due to many parameters involved during an electrochemical etching of Si, it is difficult to control its porosity. The objectives could be achieved by understanding the mechanism and process involved during the reaction. The above matter inspires me to undertake the study using n-type Si (0.0018-0.018 Ωcm) to investigate the PS formation at higher current density, effect of etching time and so on.

2.4 Morphological Characteristics of PS

Morphology is commonly defined as distribution of matter in space [30]. As for PS, it is very difficult to systematically characterize the morphology due to its extremely rich details with respect to the range of variations in pore size, shape, orientation, branching, interconnection and distribution. The morphological features are usually demonstrated in the form of images taken by Scanning Electron Microscopy (SEM). Unfortunately, it is not systematically analyzed with respect to the various morphological aspects. In 2001, Zhang [31] has systematically summarized the diverse morphological features of PS as shown in Figure 2.4. The morphological features cover four different aspects namely orientation of pores, fill of pores, branching and depth variations. The summary of morphological characteristics of PS is shown in Table 2.1.

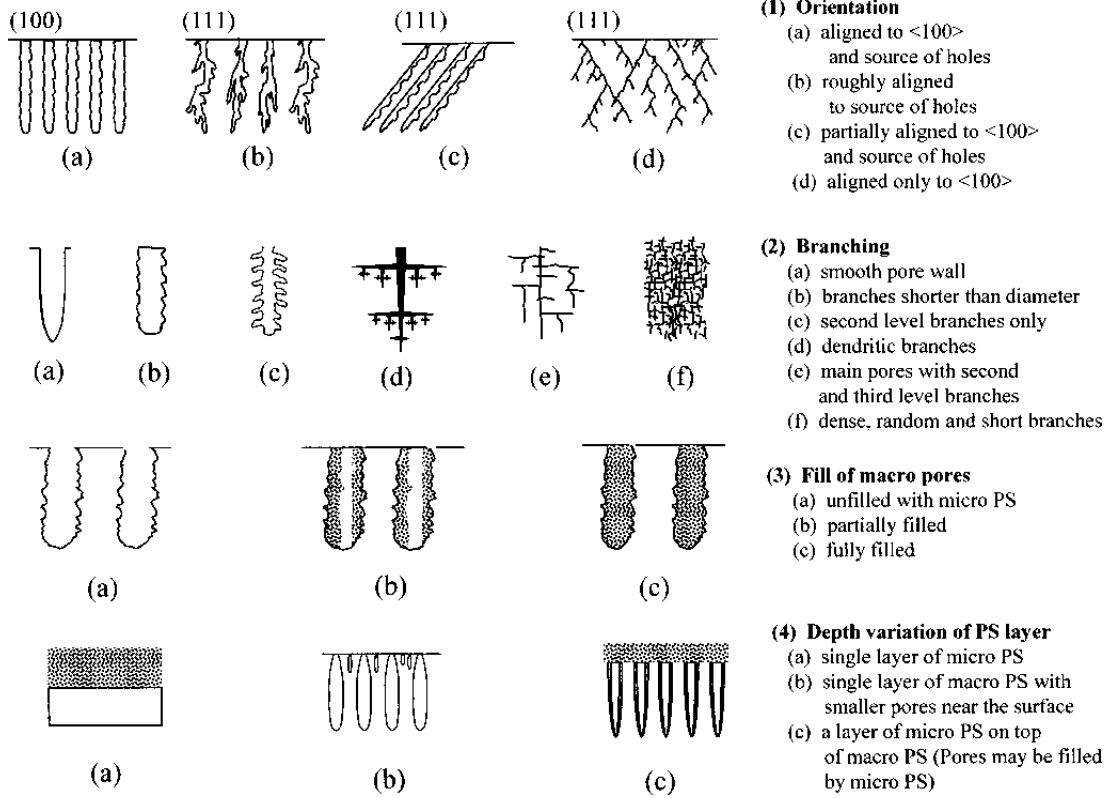


Figure 24: Morphological characteristic of PS [30, 31].

Table 2.1: Morphological characteristics of PS [30].

Size	1.	A PS layer may have one or two distinct distribution of pores with sizes varying from 1 nm to 10 μm . Those <10 nm are micropores and those >50 nm are macropores.	
		In the dark	Illumination
		-Moderately doped p-type Si (10^{15} - 10^{18}); one distribution, 1 - 10 nm -Heavily doped p- and n-type Si ($> 10^{19}$); one distribution, 10 - 100 nm -Non heavily doped n-type Si ($<10^{18}$); one distribution, 10 nm - 10 μm -Low doped p-type Si ($<10^{15}$); one or two distributions, 1 - 10 nm and > 1 μm	-Little effect on p-type Si -For n-type Si, one or two distributions, 1 - 10 nm and 50 nm - 10 μm
	2.	For p-type Si, pore diameter increases with doping concentration; for n-type Si, it decreases with doping concentration.	
	3.	It increases with potential or current density but decreases with HF concentration.	
	4.	Branched pores are smaller than primary ones.	
Orientation	5.	It is constant in the bulk but its smaller near the surface.	
	6.	Inter-pore distance can be smaller than pore diameter but is not larger than twice the diameter. It varies with the factors similar to pore diameter.	
	1.	Pores grow preferentially along <100> directions and toward the source of holes.	
	2.	Well aligned macropores, > 50 nm are perpendicular to the surface for (100) substrate but may have a less than 90° angle to the surface on other substrates.	
Branching	3.	Pores can be fully aligned with <100> directions or/and with the source of holes. Pores with a smooth wall tend to be aligned with the source of holes, while dendritic pores are aligned in the <100> direction.	
	4.	Very small pores, < 10 nm, do not show clear orientation.	
	1.	PS has discrete pores with no branches, with short branches, or with dendritic branches, or have no primary but densely and randomly branches pores.	
Fill of pores	2.	Tendency to branch increases with decreasing pore diameter.	
	3.	Direction of branching has the same tendencies as pore orientation.	
	1.	In PS of two distributions, macropores may be partially or fully filled by micropores.	
Depth variation	2.	It tends to occur in organic solvents; addition of water reduces the extent of filling.	
	3.	Extend of filling decreases with increasing light intensity or increasing potential.	
	1.	Two types, transitional layer, which has no clear boundary with the bulk, and two-layer type with a clear boundary between micro- and macro-PS layers.	
	2.	Transitional layer is associated with the initiation of pores with smaller pores at the surface.	
Others	3.	Two-layered PS occurs only on low doped p-type Si and illuminated n-type Si.	
	4.	Pore diameter and distribution is uniform in the bulk of PS.	
	1.	The bottom of pores is curved with the smallest curvature at the tips.	
	2.	The shape of pores can be square, dendritic, circular and star-like.	
	3.	Interface of PS/Si is flat and is parallel to the source of holes.	
	4.	PS with macropores has the same composition and crystalline structure as the substrate; PS with micropores can be amorphous and highly hydrogenated and/or oxidized.	
	5.	Pore wall is rough at atomic scale for all types of PS.	

In general, the morphology of PS exists in either interconnected network or columnar structure. Typically, the interconnected network morphology shows luminescent property [3, 11]. This makes PS is significant for the fabrication of electroluminescent solid-state devices. Moreover, a single layer PS consists of this particular morphology also can be used as anti-reflection coatings for solar cell. Another remarkable morphology of PS is the columnar structure. The straightness of its pores makes it a perfect template for forming other materials with the same geometric precision [11]. This is employed in the fabrication of anti-scatter grids for radiology application. In addition, it is also can act as a host for metal deposition whereby this morphology allows easier penetration of metal into the pores.

Based on the literature, the PS formed from p- and n-type Si has distinct differences in terms of pore size, orientation and degree of branching [30, 31]. A striking difference also was obtained if the Si was illuminated from the front or backside or without illumination during PS formation. However, among all the formation conditions, the doping concentration shows the clearest functional effect on morphology. In particular, the pore size depends on dopant type and concentration. For p-type Si, it increases with the increasing of doping concentration, while an opposite trend is observed for n-type Si [30].

2.5 Methods of PS Fabrications

To date, there are many methods available to fabricate PS. The easiest way is stain etching [32-43], an electroless process which only requires the Si wafer to be immersed in HF solution. It was reported that the physical structure of those layers obtained by stain etching was similar to the one fabricated by electrochemical etching. The resulting pores were usually in the range of 1 nm up to micrometer.

However, the disadvantages of the PS formed by stain etching are deficient in homogeneity, poor reproducibility and low PL efficiency. Another interesting method involving electroless deposition is chemical vapour etching. By using this method, the formed PS is mostly used as emitters in solar cell since its produce high conversion efficiency.

Spark processing [44] and reactive ion etching [45-47] also has been used to produce PS. Based on literature, all these methods can form PS, however, the as-formed PS does not reach a stage of maturity due to limitations on reproducibility, as can be obtained by electrochemical etching. In contrast, the electrochemical etching is a controllable process. It provides reproducible parameters and high quality of PS. Besides its simplicity in preparation method and is inexpensive, it is also possible to design the required structures using electrochemical etching compared to other methods. Below summarizes of PS fabrication methods.

2.6 PS Formations via Electrochemical Etching

Electrochemical etching is a conventional method widely used in producing PS. A simple electrochemical cell employs Si anode and platinum cathode in HF electrolyte. Dissolution of Si begins as soon as Si substrate is exposed to HF electrolyte. The dissolution process is accelerated by passing the electric current through the cell. Constant direct current (DC) is regularly used in electrochemical etching to ensure steady concentration of HF at the tip of the PS. As a steady concentration is achieved, the dissolution processes will be uniform and results in the formation of PS with better homogeneity.

2.6.1 Principles PS Formations

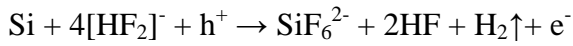
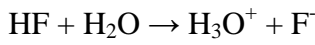
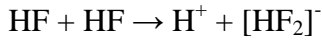
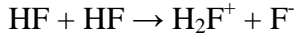
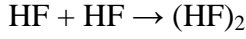
2.6.1.1 Etching Reactions

Electrochemical technique is widely used in producing PS. The main process involves is an electrochemical dissolution of anodic Si electrode in HF electrolyte. The earliest model for dissolution of Si is proposed by Gerischer et al. [48] in 1988 where the process is based on fluoride-terminated Si surface (Si-F). However, there is not enough evidence to support the proposed mechanism because no Si-F characteristic is observed in the IR spectra except for the hydride (Si-H) on the surface of PS which contradicts the fact that Si-F (6 eV) bond is more stable than Si-H (3.5 eV) bond. Thus it is unwise to simply assume that Si-F has been replaced by Si-H. Therefore, one possibility is that the Si atom readily dissolves when it is bonded to F. The Si-F bond induces a strong polarization effect therefore weakening the underlying bulk Si that is eventually attacked by HF. A generally accepted notion is that polarization encourages dissolution of Si in the presence of HF molecules.

In 1991, Lehmann et al. [2, 48] has extended the first model of Si dissolution to explain precisely the process. It provides more details about dissolution mechanism involving the fluoride-terminated Si. Two types of dissolution processes were suggested *viz.* direct dissolution and indirect dissolution. It is believed that direct dissolution occurs at low anodic potential while at high anodic potential an indirect dissolution takes place. However, the occurrence of these reactions is strongly influenced by the critical current density (J_{ps}). When the applied current density is high than the J_{ps} , indirect dissolution occurs which leads to electro-polishing and *vice versa*.

2.6.1.2 Direct Dissolution

Figure 2.5 shows the reaction scheme of PS formation via direct dissolution. The chemical equations respectively representing the reaction scheme in Figure 2.5 are as follows:



Firstly, attention is given to the initiation of the dissolution process by introducing the role of hole (step 1). Hole results from electron jumping towards the Si-electrolyte interface and transform Si atom to an electrophile. This is the rate-limiting step of the reaction and the origin of pore formation. Hence, it is susceptible to a nucleophilic attack by the active species in the electrolyte. The active species in the electrolyte is HF, its dimer $(\text{HF})_2$ or bifluoride $[\text{HF}_2]^-$. The $(\text{HF})_2$ is formed when a HF molecule reacts with another HF molecule and a reaction between a HF molecule and an F^- ion produces $[\text{HF}_2]^-$. The latter dissociates into HF and F^- ions near the surface. As the first Si-F bond established, it is immediately followed by a second nucleophilic attack upon injection of an electron (step 2). As a result of the reaction, hydrogen escapes as gaseous H_2 (step 3). Meantime, the two Si-F bonds polarize the adjacent Si bond which is readily broken by the nucleophiles (step 4). The remaining Si surface atoms area are hydrogenated (step 5) producing SiF_4 . The resultant product, SiF_4 , would react with two HF forming SiF_6^{2-} and two H^+ ions remain in the solution.

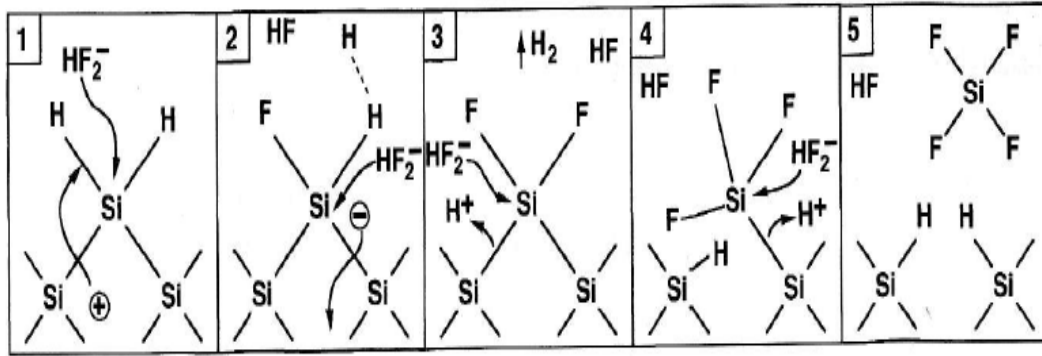


Figure 2.5: Reaction scheme for PS formation via direct dissolution [2, 48].

2.6.1.3 Indirect Dissolution

Alternatively, dissolution of Si can occur via indirect dissolution. The reaction scheme is shown in Figure 2.6. This reaction can be divided into electrochemical oxide formation (step 1 and 2) and chemical dissolution of the oxide (step 3 and 4). In the former reaction, the hydroxyl (OH^-) ion is assumed to be the active species in the electrolyte. The OH^- originates when high potential is employed during the electrochemical etching. Due to the applied potential also, it is possible for OH^- ions to diffuse through the oxide film at the interface and establish Si-O-Si bridge with the consumption of two holes. The presence of holes has created electrophilic centre of Si and causes nucleophilic attack of OH^- ion (step 1). During the reaction, the hydrogen atom which is bonded to the oxygen atom in OH^- ion escapes as H^+ ion resulting in formation of an Si-O-Si bridge (step 2). The process eventually produces anodic oxide film. As the oxide film formed, the latter reaction takes place. The oxide film dissolves chemically through nucleophilic attack on Si by fluorine that originally from either HF, $(\text{HF})_2$ or $[\text{HF}_2]^-$ (step 3). Meanwhile, an electrophilic attack of H^+ ions occurs on the oxygen bonded to the Si that results in the formation of Si-OH bond (step 4). This is the rate-limiting step and initiates

electro-polishing process. The process does not involve H_2 gas evolution due to the participation of H^+ ions in the reaction.

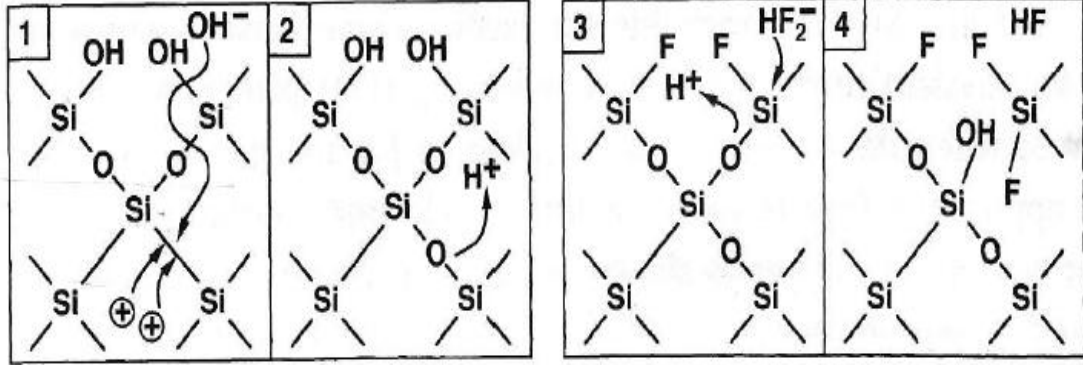


Figure 2.6: Reaction scheme for PS formation via indirect dissolution [2, 48].

2.6.1.4 Critical Current Density (J_{PS})

Both mechanisms for the dissolutions of Si are widely accepted and practical to explain most of the PS formations. However, the transition between the two dissolution processes is demarcated by a threshold quantity called critical current density (J_{PS}). Particularly, J_{PS} is defined as a crossover from a charge supply limited reaction which refers to direct dissolution at low anodic potential to a kinetically and mass transport limited reaction attributed to indirect dissolution at high anodic potential. The charge in the former case refers to the holes in the Si electrode. In the latter case, mass refers to the transportation of HF and H_2O molecules and their ionic form in an electrolyte. According to Lehmann [20], J_{PS} can be calculated from the following equation:

$$J_{PS} = C \cdot c^{1.5} \cdot \exp\left(\frac{-Ea}{kT}\right) \quad (\text{Equation 2.1})$$

where the constant C is 3300 A cm^{-2} , c is HF concentration, the activation energy E_a is 0.345 eV , k is the Boltzmann constant ($1.38 \times 10^{-23} \text{ m}^2 \text{ kg s}^{-2} \text{ K}^{-1}$), and T is the temperature.

2.6.1.5 Electro-polishing

Electro-polishing is defined as a process resulting from indirect dissolution in which causes the PS layer to detach from the bulk Si [29, 49]. It was found that electro-polishing of Si is possible to occur during PS formation if the applied anodic potential is sufficient to produce current densities in excess of the critical value (J_{PS}).

2.6.2 Si-electrolyte Interface

Studies have shown that the Si-electrolyte interface comprises of three charged layers [31]. The schematic illustration of the charged layers at the Si-electrolyte interface is shown in Figure 2.7. On the Si side, the charge layer is referred as space charge region (SCR). While on the electrolyte side it comprises of the Helmholtz and Gouy-Chapman layers.

The SCR is characterized by a band bending across. This region comprises of immobilized charge carriers originated from ionized dopants. The layer may extend to several tenth of microns in thickness into the bulk Si. Meanwhile, the mobile charge carriers in Si are electrons and holes. Ionized dopants, electrons and holes combined to give a net charge effect to the Si interface immersed in HF electrolyte. The corresponding charge state at the Si surface is depletion, inversion or accumulation. The depletion layer is formed when the surface region is depleted of majority

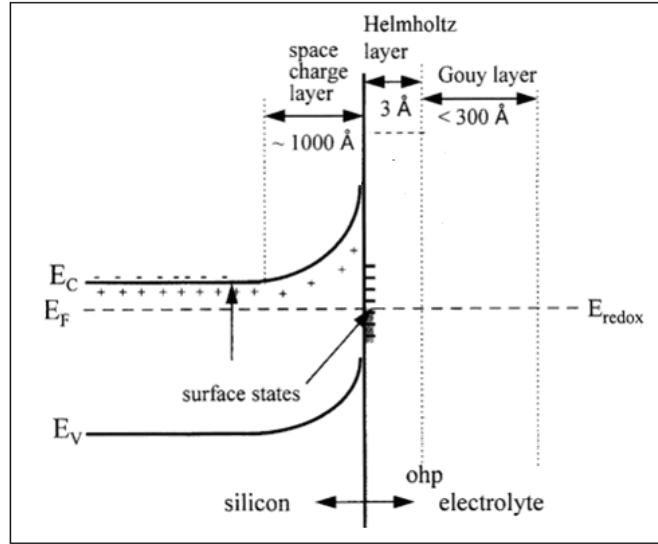


Figure 2.7: Schematic illustration of the double layers in the semiconductor-electrolyte interface at an equilibrium condition.

carriers, due to positive band bending for n-type Si or negative band bending for p-type Si. It has no mobile carriers but has immobile charges associated with the ionized dopants. The depletion layer of n-type Si is shown in Fig. 2.8(a). An inversion is formed under a depletion condition, when the minority carriers accumulate near the surface and in equilibrium with those in bulk Si as shown in Figure 2.8(b). Meanwhile, the accumulation occurs when the excess of the majority carriers due to injection of electrons into n-type Si or holes into p-type Si accumulate at the surface and cause the band bending in this layer as shown in Figure 2.8(c).

On the other hand, ions are the mobile charge carriers in an electrolyte. The Helmholtz layer is formed by ions and molecular dipoles attracted to the Si surface by the excess charge in the SCR. The layer is subdivided into outer Helmholtz plane (OHP) and inner Helmholtz plane (IHP) with the latter sandwiched between OHP and

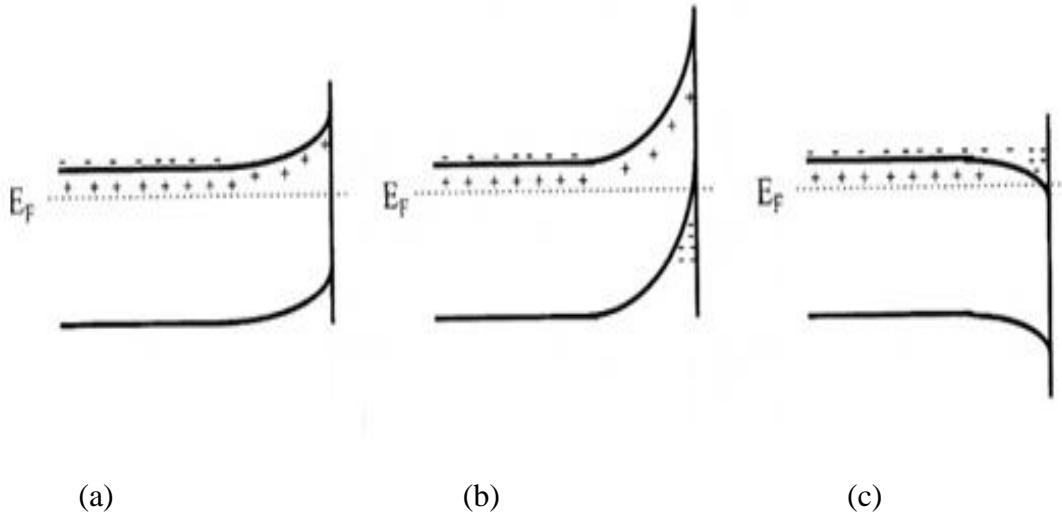


Figure 2.8: Types of space charge layers on n-type Si surface (a) depletion, (b) inversion and (c) accumulation layer [31].

Si surface. The layer contains electrolyte molecules and sometimes other specially adsorbed species such as H^+ , OH^- and F^- . Beyond OHP is the Gouy-Chapman layer that comprised of excess anion or cation whose thickness depends on the electrolyte concentration. Generally, as the concentration of electrolyte increases ($> 0.1\text{ M}$), the role of the Gouy-Chapman layer is negligible [31]. The actual thickness of these overall layers is controlled by several factors such as dopant loading, surface state and surface defect in the electrode Si, electrolyte concentration and applied potential. Moreover, the surface states, adsorbates or surface defects are also important in determining the distribution of charge in the depletion region. Occasionally, the reaction processes at the electrodes result in the formation of oxides on the Si surface. This oxide layer on the Si surface can affect the electrical properties of the Si-electrolyte interface, however, depending on its thickness and degree of homogeneity.

2.6.3 Parameters Controlling the PS Formations

During PS formation by electrochemical etching, there are many parameters that may influence the process of dissolution. As previously reviewed [42], the parameters include current density, etching time, HF concentration, pH of electrolyte, temperature, illumination, dopant types, dopant loading and Si orientation.

2.6.3.1 Current Density

Current density is defined as the numbers of flowing charges per unit area. In this case, the charge refers to the mobile electrons in Si electrode and ions in an electrolyte. In SI unit, it is written as $A\ m^{-2}$. Movement of the charges in a closed circuit generates holes that orient in an opposite direction to electrons in the Si electrode, whereby the quantity is dependent on the applied current density. Typically, as the current density increases, the number of holes increased as well. While holes are crucial to the dissolution of Si, their quantities influence the kinetics of the process. Due to the role of holes in the dissolution of Si, therefore the etch rate of Si increases with the increasing of current density.

2.6.3.2 Etching Time and HF Concentration

The etching time is defined as the time taken during the occurrence of anodic reaction at the Si-electrolyte interface. The longer the etching time translates to the longer residence of Si substrate in the HF solution. This causes the mass of chemically dissolved Si becomes higher which result in the formation of thicker PS layer [42, 50]. In this case, the mass transfer during the etching process should be taken into account [42, 51]. In order to obtain vertical homogeneity of PS layers, two

different aspects have to be considered. These aspects are the chemical dissolution of Si in the electrolyte and the changes in the HF concentration during the anodization process. Canham [1] and Lehmann [2] suggested that the dissolution is restricted by the carrier's transport i.e. holes in the PS structure and by mass transport of the reactants i.e. HF and its ionic form through the pores, which follows Fick's law:

$$F_{\text{HF}} = D_{\text{HF}} (C_{\text{top}} - C_{\text{bot}}) / d \quad (\text{Equation 2.2})$$

where F_{HF} is the flux of the HF molecules ($\text{mol m}^{-2} \text{ s}^{-2}$), D_{HF} is the diffusion coefficient of the molecules into the pores, C_{top} and C_{bot} refer to the HF concentrations at the top and bottom of the PS layer, correspondingly. Meanwhile, d is the layer thickness. Thus, for deep pores, resulting from long etching time, the diffusion effect is important. As the pore depth increases, the diffusion of molecules into and out of the pores becomes more difficult. On the other hand, the holes diffusion at the pore tip becomes easier as the distance between the pore tip and the bulk Si decreases especially if the Si is illuminated from the backside. There is ~20% difference in HF concentration between the tips of pores and the bulk solution for a very thick PS layer ($d = 150 \mu\text{m}$) as reported by Lehmann [20].

In fact, the effects mentioned above may change the current density and J_{PS} [42]. Therefore, if the current density is kept constant during an etching experiment, this will not necessarily keep the pore diameters constant. For a fixed thickness of PS layer, the reduction of HF concentration from top to the bottom will be larger when the applied current density is higher. This means that longer etching time will cause a porosity gradient. It indicates that there is a reduction in the growth rate of pores due to the decline of etch rate of direct dissolution at pore tip. However, the etch rate of

indirect dissolution at the pore wall is increased. Therefore, the diameter of deep pores may increase due to the effect of diffusion process in the pores. The depth where this occurs is dependent on the current density value and the HF concentration [52]. However, the low etching rate and low temperature will lead to the formation of uniform deep pores.

On the other hand, referring to equation 2.1, the HF concentration is proportional to the J_{PS} . As the HF concentration increases, the J_{PS} increase as well even at constant current density. Therefore, the large difference between the current density and J_{PS} exists and caused the etch rate of direct dissolution of Si at pore tip to become high at high HF concentration and *vice versa*.

2.6.3.3 Temperature and pH of Electrolyte

The temperature of electrolyte is also a significant parameter on the formation of PS. However, studies that have been published are inadequate. According to equation 2.1, the J_{PS} increase with the increasing temperature of electrolyte at constant current density [53]. This induces large difference between current density and J_{PS} . Hence, the etch rate at pore tip should increase with increasing temperature.

Meanwhile, for the influence of pH, the etch rate increase as the pH value is increased [20, 42]. The increment of etch rate is due to the increasing level of OH^- ions in the electrolyte with the enhancement of pH values. These OH^- ions promote chemical dissolution of the PS branches. Dissolution continues for as long as the PS remains in contact with the electrolyte thus increasing the porosity even after anodization is completed. However, the dissolution rate is partially dependent upon the surface area available for reaction.

2.6.3.4 Types of Dopant, Dopant Loading and Illumination

Dopant also contributes to the availability of holes in Si substrates. In the p-type Si, holes are in excess where higher dopant loading increases the number of holes. In contrast, the availability of holes in the n-type Si is scarce. Therefore, the etch rate increases with the increase in dopant loading for p-type Si which is the opposite for n-type Si. Normally, an external source of illumination is used to generate excess holes in the n-type Si electrode during electrochemical etching of Si.

2.6.3.5 Si Orientation

In crystalline Si, atoms are arranged in three orientations, namely $\langle 100 \rangle$, $\langle 111 \rangle$ and $\langle 110 \rangle$. Due to similar polarizing effect on the bulk of Si by the surface of Si-F and Si-OH, such anisotropy has been shown to influence direct dissolution of Si depending on the Si orientation. Thus, $\langle 100 \rangle$ orientation enhances the kinetics of dissolution of Si compared to $\langle 111 \rangle$ and $\langle 110 \rangle$ due to steric effects. However, there is no dependence on orientation for dissolution via indirect dissolution.

2.6.4 Properties of PS Formed by Electrochemical Etching

2.6.4.1 Crystal Structure

Many reports have shown that the crystal structure of PS is similar to its bulk, i.e. Si single crystal [54-56]. However, some evidence also showed the presence of amorphous regions [57]. However, the amount of amorphous layer varies with oxidation, ageing and post-anodization treatment.